Catalysis Letters 27 (1994) 221–233

# Electrochemical methane conversion over $SrFeO_{3-\delta}$ perovskite on an yttrium stabilized zirconia membrane

Arnfinn G. Andersen [1]

*Section of Hydrocarbon Process Chemistry, SINTEF, PO Box 124 Blindern,*
*0314 Oslo 3, Norway*

Takashi Hayakawa [1], Kunio Suzuki, Masao Shimizu and
Katsuomi Takehira [1]

*Oxidation Laboratory, Department of Surface Chemistry,*
*National Institute of Materials and Chemical Research*
*(National Chemical Laboratory for Industry), Tsukuba Research Center,*
*AIST, 1-1 Higashi, Tsukuba, 305 Ibaraki, Japan*

Received 24 August 1993; accepted 20 April 1994

Oxidative methane coupling and the related chemical reactions have been studied in an electrochemical membrane cell of the type: $CH_4$, $(O_2)$, $SrFeO_{3-\delta}$, Au|8%$Y_2O_3$ : $ZrO_2$|Ag, air. The results are compared to a fixed bed study of $SrFeO_{3-\delta}$. The $C_{2+}$ selectivity and the alkene/alkane ratio may be higher in the cell reactor than in the fixed bed reactor, but the $C_{2+}$ yield never exceeded fixed bed data. The maximum $C_{2+}$ yield observed in the cell reactor was 3.1%. The electric fields in the cell when electrodes were connected influenced the selectivity to $CO_2$ in a manner which may be related to the NEMCA effect.

**Keywords:** methane conversion; electrochemical membrane reactor; perovskite

## 1. Introduction

Oxidative coupling of methane ($CH_4$) is an attractive process for producing $C_2$ hydrocarbons, and many studies have been done in this field since Keller and Bhasin first demonstrated this possibility [1–4]. It is generally accepted that the initial step in the catalytic oxidative coupling of $CH_4$ (OCM) involves the homolytic cleavage of a C–H bond on the catalyst surface to form $CH_3\cdot$ radicals which may undergo coupling to form ethane in the gaseous phase [5]. The intermediate radicals and the products may undergo deep oxidation to carbon oxides in the pres-

---

[1] To whom correspondence should be addressed.

ence of molecular oxygen. It has therefore been frequently proposed to use the cyclic operation by feeding methane and oxygen alternatively over the catalyst interspaced by a short purge of inert gas [4] or to use an oxygen permeable membrane [6].

The present study contains several experiments on a catalyst for electrochemical conversion of light hydrocarbons, using a zirconia solid electrolyte membrane reactor. The reactor has been described by several authors [7,8]. A catalyst for this purpose should have the following properties: (1) The catalyst should be mechanically and chemically stable during operation under reaction conditions. (2) The catalyst should be able to activate hydrocarbons, and show significant selectivity. (3) To be able to use the catalyst in an electrochemical reactor, the catalyst should have considerable conductivity for both electrons and oxide ions. (4) If possible, the material should have thermal properties that match the substrate $ZrO_2$ fairly well. The material characteristics mentioned above are found among some perovskites, and titanates are among the most stable compounds of this class.

A recent report by Xu et al. [9] showed that the perovskite $Ca_{0.9}Sr_{0.1}TiO_3$ has reasonably high catalytic activity for oxidative coupling of methane in a fixed bed reactor. Interesting results on the same reaction with perovskite oxides have also been obtained in a TPR reactor [10]. In the study by Xu [9] the lifetime of the catalyst was tested for 500 h with no significant loss of activity. Analysis showed no change in the catalyst during this period. In this respect perovskites may have interesting properties compared to OCM catalysts containing alkaline and alkaline earth metals [2,3].

In the OCM reaction by using the electrochemical reactor, it is expected that electrochemical oxygen pumping through the solid electrolyte affects the oxidation results over the surface of catalyst. Vayenas and coworkers [11–13] have recently reported that catalytic activity may actually be promoted as the electronic work function of the catalyst is influenced by the potentials in the electrochemical reactor; this is often referred to as the non-faradaic electrochemical modification of catalytic activity (NEMCA) effect.

We have previously reported on the synthesis of a large number of perovskites [14], as well as on their fixed bed testing as the catalyst for oxidative coupling of $CH_4$ [25] and oxidative dehydrogenation of ethane [17]. The present work describes the behavior in the electrochemical reactor of the material among previously reported catalysts which is presumably optimal with respect to the criteria mentioned above.

## 2. Experimental

Discs of 8% $Y_2O_3 : ZrO_2$ (Nikkato), diameter 31.5 mm, thickness 1.0 mm were rinsed in distilled water in an ultrasonic bath, and calcined for 5 h at 1173 K. Two gold leads (0.1 mm diameter) were fixed on the anode side of the disc with gold paint (Tokuriki kagaku No. 8570) and fired 10 min at 1273 K; this high temperature was important in order to prevent spalling of the leads after introduction of the perovskite. On the cathode side, a gold lead was fixed with silver paint (Fujikura kasei, DOTITE K-1058), which was dried before the rest of the silver cathode was painted on this side of the disc. The cathode was fired 10 min in air at 1023 K. The conductivity in the cathode was checked in several points on the surface by a multimeter, which showed no detectable resistance in this layer. The cathode thus produced consisted of a silver layer of approximately 5 μm.

A mixture of 25 mg of a prepared perovskite powder ($SrFeO_{3-\delta}$) and 80 mg of gold paint (yielding 40 mg Au after heating) was painted on the anode side of the disc, and fired 10 min in air at 1023 K. Details on the synthesis and characterization of this perovskite can be found elsewhere [14]. Finally, each cell was vacuum sealed in a polymer envelope and treated for 10 min at 200 MPa in a Cold Isostatic Press (CIP). This treatment is supposed to enhance the contacts between different phases on the anode side of the cell. Without the CIP treatment, identical cells lost much of their conductivity in the anode after few hours of operation. The active area of the disc was about 4 $cm^2$. Scanning electron microscopy of the anode surface showed a good dispersion of gold, perovskite and pores. According to the images, as well as conductivity measurements at room temperature, there was probably a continuous, thee-dimensional network of gold in the anode. The cells produced in this way have no reference electrode. However, two leads to the anode ensured that we could check the conductivity in the anode during operation. In addition to ohmic resistance, we expected chemical overpotentials only on the anode side of the cells.

The cells were mounted between two vertical alumina tubes and sealed with a slurry of pyrex glass powder in water. The temperature was increased up to 1123 K with air in both anode and cathode chambers, and the absence of leaks was confirmed by a pressure regulator tube, giving an overpressure corresponding to 60 cm of water. Experiments were started when no pressure drop was observed after 1 h holding time.

The anode chamber was flushed with $N_2$ before $CH_4$ (Takachiko Chemical Industry Co., Ltd. 99.99%) was introduced. Except when specifically mentioned in the text, the flow rate of methane was 1500 ml/h. In the cathode chamber, 1200 ml/h of air flow was used. Product gases were gathered from the cell surface and led out through a thin quartz tube with a small dead volume. Samples of 0.5 ml of product gases were analysed by gas chromatography. Water was not quantitatively analysed in this study. The reactor system and the electrical measurement equipment have been described elsewhere [8].

## 3. Results and discussion

### 3.1. CELL PROPERTIES

The resistance across the cell was measured by a multimeter with air in both the cathode and anode chambers, giving 3.5, 2.5, 1.6 and 1.3 Ω at 973, 1023, 1073 and

1123 K, respectively. In the outer circle, for measurements referred to as "closed circuit", without externally applied potential, the resistance was 2.5 Ω. One cell which had been in continuous operation for 15 days was carefully dismounted for characterization. The resistivities checked in several points on the surfaces were still undetectable by multimeter. The anode surface was studied by XRD, which showed lines from the perovskite, $SrFeO_{3-\delta}$, and gold. Weak lines from the underlying zirconia could also be seen, but decomposition of the perovskite was not observed. The anode surface was also studied by scanning electron microscope (SEM), and one micrograph is shown in fig. 1. There are pores in the anode, and gold and perovskite particles are still well dispersed.

An open cell voltage with 1500 ml/h methane flowing in the anode chamber was observed at 1.2 eV. This figure is not the ultimate open circuit voltage, as we did not allow equilibrium to be established in the open cell mode with pure methane in the anode chamber. This could easily cause irreversible reduction of the catalyst.

### 3.2. MEASUREMENTS IN METHANE

Based upon the measurements of Vayenas [11] and others the reaction rate on a 4 $cm^2$ area of YSZ without a catalyst is expected to consume $2 \times 10^{-9}$ (mol $CH_4$)/s

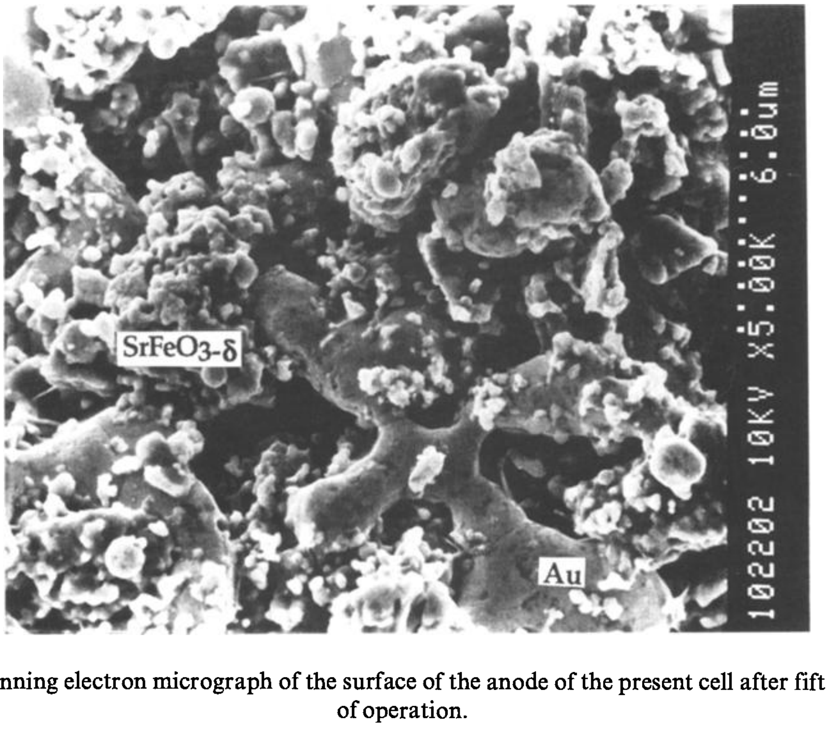

Fig. 1. Scanning electron micrograph of the surface of the anode of the present cell after fifteen days of operation.

under conditions similar to the present study. The observed rates in this study are typically two to three orders of magnitudes higher, and are thus dominated by the effect of the catalyst.

External potentials of 0, 0.1, 0.25, 0.5, 1.0 and 2.0 V were applied to the cell, and the electric characteristics of the cell at four temperatures with a flow of 1500 ml/h of methane in the anode chamber are shown in fig. 2. The points at the lowest current were measured by replacing the potentiostat by a copper wire. The total resistivity in the wiring between anode and cathode was 2.5 Ω. From the measurements in fig. 2, an average resistance in the range of 0–2 V applied voltage at the various temperatures is calculated to be 13, 6.0, 4.1 and 4.0 Ω at 973, 1023, 1073 and 1123 K, respectively. The data at 973 K showed an increasing resistance with applied potential, indicating a chemical limitation.

The resistances are higher with methane in the anode chamber than the similar data with air in both chambers as given above, even if the ohmic resistance measured by the two leads in the anode was unaffected. We assume this is due to the conductivity of the perovskite, as chemical reactions (oxygen exchange in air and methane conversion in methane) take place over the whole surface of the perovskite. $SrFeO_{3-\delta}$ is a good p-type conductor in high oxygen partial pressures; the conductivity decreases at lower oxygen partial pressures [18]. Thus, surface far from the three phases boundaries (perovskite, gold and gas) will experience an increased resistivity due to lower ionic and electronic transport when air is replaced by methane in the anode chamber. In effect this means that a larger surface area of the perovskite will be electrochemically active in air than in methane atmosphere. The total surface area of the perovskite used in the electrode is approximately 250 $cm^2$.

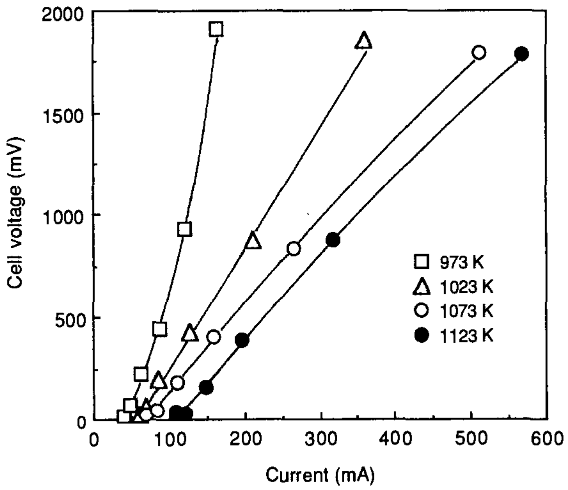

Fig. 2. The potential across the membrane at various temperatures as a function of the current through the membrane.

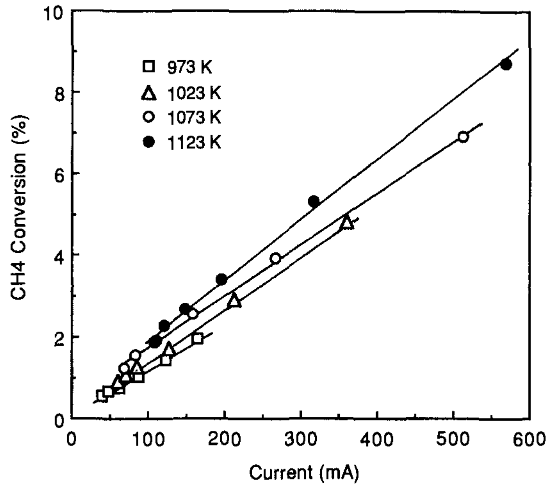

Fig. 3. Methane conversion at various temperatures as a function of the current in the membrane.

The methane conversions at various temperatures are illustrated in fig. 3. The conversion increased with temperature and current in the membrane. No oxygen was detected in the GC analysis, therefore oxygen conversion was close to 100% in all the experiments. To compare the oxygen feed through the membrane with the 1500 ml/h methane flow one should remember that 1 A equals an oxygen flow of 209 ml/h at STP. At 1 A deep oxidation to only $CO_2$ and $H_2O$ would lead to 7% methane conversion. When taking the selectivity to $C_{2+}$ compounds into account, the methane conversion will be higher, corresponding to the data in figs. 3 and 4. The oxygen mass balance is well accounted for by assuming water as the only compound which is not analyzed.

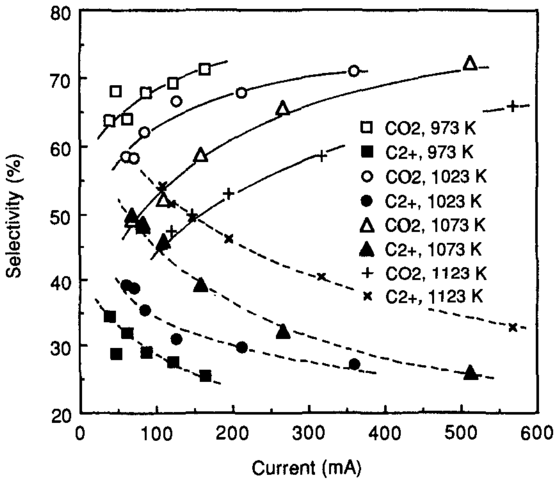

Fig. 4. Selectivity to $CO_2$ and $C_{2+}$ at various temperatures as a function of current in the membrane.

The selectivities of the reaction are shown in fig. 4. The main products are $CO_2$, $H_2O$, ethane and ethene. The CO selectivity was nearly constantly 1–3% and is not included in the figure. The selectivity to higher hydrocarbons increased with temperature and decreased with current. A small amount of $C_3$ compounds (approximately 5% of the $C_{2+}$ compounds), and at high conversions traces of $C_4$ compounds were observed. The alkene/alkane ratio is illustrated in fig. 5 as a function of current. The data are not directly comparable, as they are taken at widely different applied voltages, but generally the ratio increased with the current, and thus with the methane conversion. The maximum yield of $C_{2+}$ compounds in this series of experiments was 2.9% at 1123 K and 2.0 V applied potential.

We have previously reported on methane conversion in a fixed bed reactor with the same catalyst in a mixture of 1500 ml/h methane and 280 ml/h of air [15]. In the present study, the same oxygen content corresponds to a current of 270 mA. A direct comparison of data can be made at 1023 K, where the fixed bed reactor showed 48% selectivity to $C_{2+}$ at 4.5% methane conversion, while the cell reactor gave 30% selectivity to $C_{2+}$ at 4.0% methane conversion. Several of the trends in fig. 4 can be recognized in the tests with variable temperature and gas mixtures in the fixed bed reactor [15]. At higher temperatures and low current, the $C_{2+}$ selectivity in the electrochemical reactor (fig. 4) was higher than any $C_{2+}$ selectivity in fixed bed reactor. However, these selectivities are accompanied by low methane conversion. The highest $C_{2+}$ yield observed in the electrochemical reactor with 1500 ml/h methane flow in the anode chamber was 2.9%, while the maximum $C_{2+}$ yield over the same catalyst in fixed bed reactor was 4.8%. Some methane may react on the surface of the zirconia electrolyte, and this material is assumed to have a certain activity for deep oxidation.

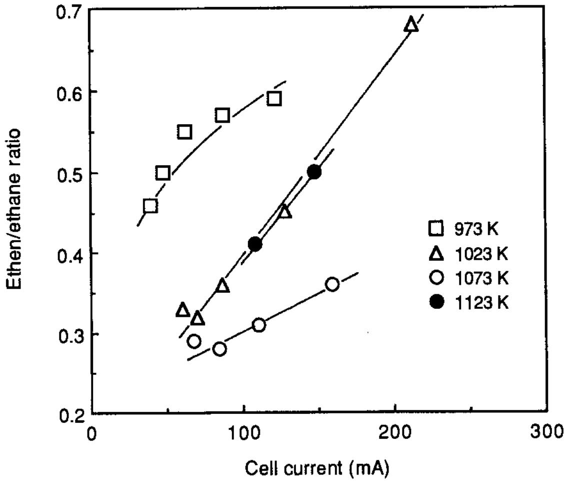

Fig. 5. Ethene/ethane ratio at various temperatures as a function of the current in the membrane.

### 3.3. MEASUREMENTS IN VARIABLE FLOW

The methane conversion was studied as a function of the flow of methane in the anode chamber at 1123 K with a closed circuit (i.e. without applied potential) and with an applied potential of 2.0 V across the membrane. With 2.0 eV applied potential, the current did not change as a function of the methane flow: the potential across the membrane was constantly 1.8 V and the current was 563 mA. The cell voltage and current for the closed circuit as a function of the methane flow are shown in fig. 6. The cell voltage, and thus also the current decreased with increasing methane flow. The total drop was about 20% in the flow range used. The selectivities to $C_{2+}$ and $CO_2$ at 1123 K as a function of methane flow over a closed circuit cell and at 2.0 V applied potential are shown in fig. 7. Higher $CH_4$ conversion was observed in 2.0 V applied potential operation than the closed circuit, while higher selectivity to $C_{2+}$ was obtained with the closed circuit operation. The CO selectivity was less than 3% for all experiments in this series. The $C_{2+}$ selectivity increased with the flow rate and decreased with applied potential at all flow rates. The alkene/alkane ratio in the $C_{2+}$ compounds decreased with the flow rate of $CH_4$ (250–1500 ml/h) and increased with applied potential (0–2.0 V). The maximum $C_{2+}$ yield of 3.1% was reached at 2.0 V applied potential and 250 ml/h methane flow rate. The alkene/alkane ratio observed in the cell with 250 ml/h of methane (1.7) is higher than any similar ratio observed in cell or fixed bed tests with this catalyst. The dependence of flow indicates alkenes are secondary products in the reaction.

The decrease in cell voltage with increasing flow was unexpected. This effect is, however, probably linked to the selectivity at various flows. At high flow rates the

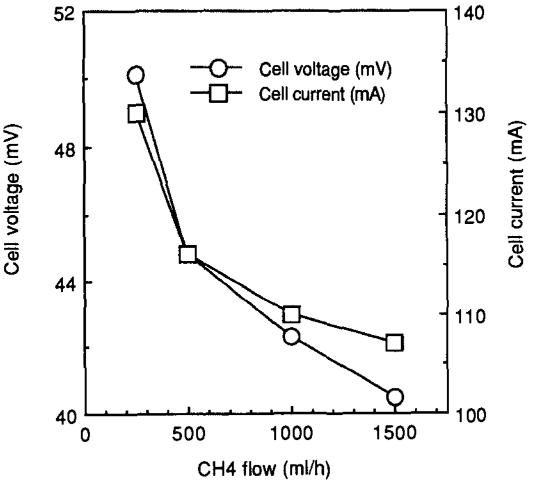

Fig. 6. The cell voltage and cell current for a closed circuit cell at 1123 K as a function of the flow of pure methane in the anode chamber.

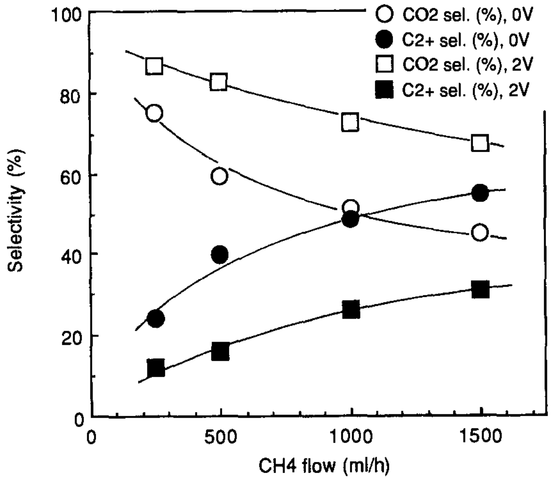

Fig. 7. Selectivities to $C_{2+}$ and $CO_2$ over a closed cell and at an applied potential of 2.0 V at 1123 K as a function of the methane flow in the anode chamber.

main products are $C_2$ and $H_2O$. At lower flow rates, $CO_2$ becomes a major product. We assume this change affects the efficiency of oxygen removal from the perovskite, and thus the cell voltage, which is given by the Nernst equation, where $P^{c}_{O_2}$ and $P^{a}_{O_2}$ are the partial pressures of oxygen at the cathode and anode, respectively:

$$E = (nF/RT)\ln(P^{c}_{O_2}/P^{a}_{O_2}) . \tag{1}$$

### 3.4. MEASUREMENTS IN DILUTED METHANE

The influence of the methane flow on the properties of the cell at 1123 K was also investigated by diluting methane in helium. The total gas flow of 1500 ml/h was kept constant, while the ratio of methane to helium was changed. The resulting cell voltage and current in a closed circuit cell are illustrated in fig. 8. There were fairly linear increases in the voltage and the current with the methane content in the gas. To relate the observations at closed circuit conditions to the discussion concerning variable flow in the previous section, one should note that the highest cell voltage in fig. 8 equals the lowest voltage in fig. 6. Dilution of methane with helium led to a reduced ability for oxygen removal from the anode and, thus a lowered cell voltage in the fuel cell mode.

The methane conversion decreased with the methane content, typical values were 3% in 50% methane and 1.9% in pure methane. The selectivities to $CO_2$ and $C_{2+}$ compounds are illustrated in fig. 9. As the methane content increased the $C_{2+}$ selectivity also increased. Maximum yield was observed with no dilution. There were negligible amounts of CO in the product stream.

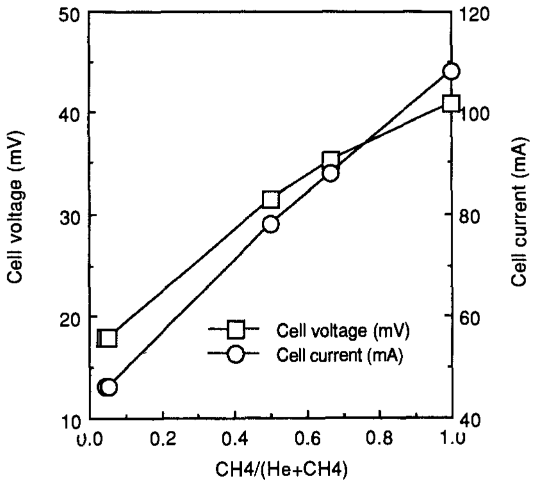

Fig. 8. The cell voltage and cell current for a closed circuit cell at 1123 K as a function of methane content in a gas mixture of $CH_4$ + He. The total flow rate was 1500 ml/h.

### 3.5. MEASUREMENTS IN GAS MIXTURES

A gas mixture of methane (1500 ml/h) and air (280 ml/h) was fed to the anode of the cell at 1123 K. The current/voltage characteristics was the same as for the cell without air (see fig. 2) at high applied voltages. At lower applied voltages, there was a deviation towards lowering the cell potential when air was added. The open cell potential was lowered from about 1.2 V in pure methane to about 0.95 eV in

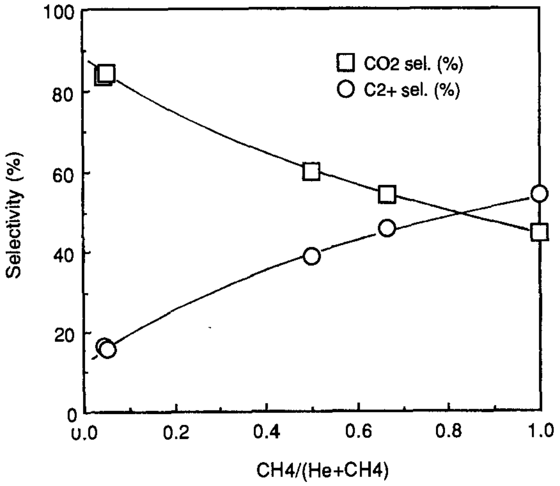

Fig. 9. Selectivities over a closed cell as a function of the methane concentration in a mixture of $CH_4$ + He.

the mixture of methane and air. The methane conversion as a function of the cell current for the mixture of methane and air is illustrated in fig. 10. Compared to the results in fig. 3, the conversion was higher in the mixed gas, especially at low cell currents. In the open cell mode, a conversion of 5% was obtained, corresponding to the reaction of methane with the oxygen fed in the gas phase. This is in fair agreement with observations in the same gas mixture in the fixed bed reactor [15], where the methane conversion was increasing with temperature, reaching 4.7% at 1073 K, which was the highest temperature used in fixed bed studies.

The selectivities to CO, $CO_2$ and $C_{2+}$ in the mixture of methane and air in the anode chamber are illustrated in fig. 11 as a function of the cell current. In the open cell mode, almost equal amounts of CO, $CO_2$ and $C_{2+}$ were obtained. As soon as the anode and cathode of the cell were connected, the selectivity to CO dropped to about 5%, that to $CO_2$ increased to 65% and the $C_{2+}$ selectivity was fairly constant at 30%. Increasing the cell current increased the $CO_2$ selectivity, while the CO selectivity decreased correspondingly and the $C_{2+}$ selectivity was not affected substantially. The selectivities at 170 mA in fig. 11 correspond well to the those at 440 mA at the same temperature in fig. 4 (440 mA in fig. 4 corresponds to 170 mA in the membrane plus 280 ml/h air added in the gas phase). These similarities indicate that there is little difference in reactivity between oxygen fed through the membrane and in the gas phase. We assume the same surface reactions are governing the reaction patterns for both types of oxygen. The maximum $C_{2+}$ yield obtained in this series of experiments was 2.4% at the extreme point of the graph in fig. 11, slightly lower than the yield obtained without air in anode gas. A possible explanation for the small electrocatalytic effect on the $C_2$ selectivity is that the mechanism

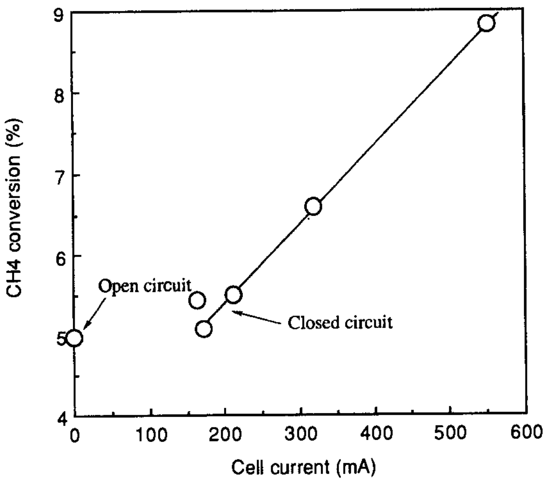

Fig. 10. Methane conversion at 1123 K in a mixture of methane (1500 ml/h) and air (280 ml/h) as a function of current in the membrane.

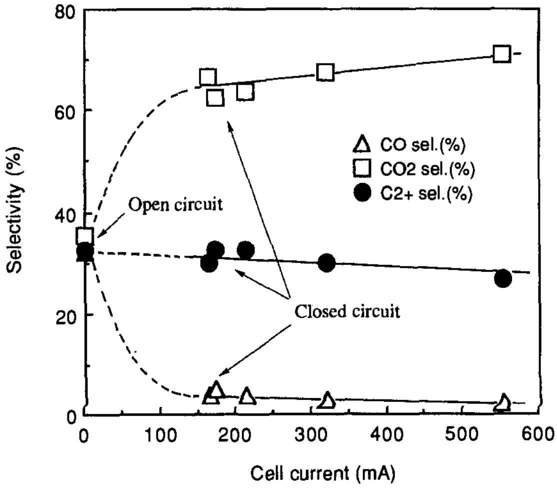

Fig. 11. Selectivities at 1123 K in a mixture of methane (1500 ml/h) and air (280 ml/h) as a function of current in the membrane.

of methane coupling involves both surface and gas phase steps. Oxygen pumping, which can only modify the surface, has limited influence on the $C_2$ selectivity.

The selectivities in the open cell mode are in good agreement with the observations in fixed bed reactor in the same gas mixture. The CO production observed here in the open cell mode, and also in fixed bed reactor [15], is probably not due to reforming reactions. Reforming catalysts normally shift the selectivities of the reaction completely to produce mainly CO and $H_2$, as seen over cobalt or nickel containing perovskite oxides [16,17]. The change in selectivities when current is allowed to pass through the cell is not comparable to results in fixed bed studies. In fixed bed studies a large increase in $CO_2$ selectivity requires a higher oxygen concentration. This is accompanied by a corresponding drop in $C_{2+}$ selectivity [15], which is not observed in the cell reactor. Thus, the sudden change in selectivities in the cell reactor when current is turned on is interpreted in terms of a promoter effect caused by the change in electronic potentials in the anode.

In NEMCA studies the specific rates of several oxidation reactions have been directly related to changes in the work function of metallic anodes [12,13]. NEMCA effect is known to promote the rate of these reactions. To the knowledge of the authors only one study of NEMCA effect on the methane coupling reaction over an oxide electrode has been published [11]. In the present study the selectivity is altered by electronic potentials. Lacking a reference electrode it goes beyond the scope of this work to elaborate on the work function of the anode materials. However, we claim that the observed relationship between selectivities and currents as seen in fig. 11 probably is related to a promoter effect caused by the electric field set up when the electrodes in the cell are connected. The nature of this phenomenon may be the same as for previously observed NEMCA effects.

## 4. Conclusion

Electrochemical cells with an anode of Au + $SrFeO_{3-\delta}$ were successfully produced and operated for extended periods of time. Conversion and selectivities of methane coupling and oxidation have been characterized over a wide range of temperatures, gas mixtures and applied potentials. The results have been compared to fixed bed studies of the same catalysts. $C_{2+}$ selectivity and alkene/alkane ratio may be higher in the cell reactor than in the fixed bed reactor, but the $C_{2+}$ yield never exceeded that in the fixed bed reactor. A promoter effect for $CO_2$ production was observed which may be related to the NEMCA effect.

## References

[1] G.E. Keller and M.M. Bhasin, J. Catal. 73 (1982) 9.
[2] T. Ito, J.-X. Wang, C.-H. Lin and J.H. Lunsford, J. Am. Chem. Soc. 107 (1985) 5062.
[3] K. Ohtsuka, K. Jinno and A. Morikawa, J. Catal. 100 (1986) 353.
[4] J.A. Sofranko, J.J. Leonard, C.A. Jones, A.M. Gaffney and H.P. Wither, Catal. Today 3 (1988) 127.
[5] E. Iwamatsu and K.-I. Aika, J. Catal. 117 (1989) 416.
[6] K. Omata, S. Hashimoto, H. Tominaga and K. Fujimoto, Appl. Catal. 52 (1989) L1.
[7] C.B. Choudhary, H.S. Maiti and E.C. Subbarao, in: *Solid Electrolytes and Their Applications*, ed. E.C. Subbarao (Plenum Press, New York, 1980) pp. 1–80.
[8] T. Hayakawa, T. Tshunoda, H. Orita, T. Kameyama, H. Takahashi, K. Takehira and K. Fukuda, J. Chem. Soc. Chem. Commun. (1986) 961;
T. Hayakawa, T. Tsunoda, H. Orita, T. Kameyama, H. Takahashi, K. Fukuda and K. Takehira, J. Chem. Soc. Commun. (1987) 780;
T. Hayakawa, T. Tsunoda, H. Orita, T. Kameyama, M. Ueda, K. Fukuda and K. Takehira, J. Chem. Soc. Chem. Commun. (1988) 1593.
[9] Y. Xu, H. Lui, J. Huang, Z. Lin and X. Guo, *Proc. 3rd China–Japan Symp. on Coal and $C_1$ Chemistry*, Kunming, 29 October–1 November 1990, p. 449.
[10] T. Hayakawa, H. Orita, M. Shimizu, K. Takehira, A.G. Andersen, K. Nomura and Y. Ujihira, Catal. Lett. 16 (1992) 359.
[11] S. Bebelis, I.V. Yentekakis, S. Neophytides, P. Tsiakaras, H. Karasali and C.G. Vayenas, *Proc. 3rd. Int. Symp. on Solid Oxide Fuel Cells*, May 1993, eds. S.C. Singhal and H. Iwahara, p. 926.
[12] C.G. Vayenas, S. Bebelis and S. Ladas, Nature 343 (1990) 625.
[13] C.G. Vayenas, S. Bebelis, I.V. Yentekakis and H.G. Linz, Catal. Today 11 (1992) 303.
[14] A.G. Andersen, T. Hayakawa, T. Tsunoda, H. Orita, M. Shimizu and K. Takehira, Catal. Lett. 18 (1993) 37.
[15] A.G. Andersen, T. Hayakawa, M. Shimizu, K. Suzuki and K. Takehira, Catal. Lett. 23 (1994) 59.
[16] T. Hayakawa, A.G. Andersen, M. Shimizu, K. Suzuki and K. Takehira, Catal. Lett. 22 (1993) 307.
[17] T. Hayakawa, A.G. Andersen, H. Orita, M. Shimizu and K. Takehira, Catal. Lett. 16 (1992) 373.
[18] T.R. Clevenger Jr., J. Am. Ceramic Soc. 46 (1963) 207;
L.H. Brixner, Mater. Res. Bull. 3 (1968) 299;
J.B. MacChesney, R.C. Sherwood and J.F. Potter, J. Chem. Phys. 43 (1965) 1907;
S. Shin, Mater. Res. Bull. 16 (1981) 299.